



OPEN Influence of mudstone on coal spontaneous combustion characteristics and oxidation kinetics analysis

Xun Zhang^{1,3}, Jiahui Zou¹✉, Bing Lu¹, Gang Bai² & Ling Qiao⁴

To explore the spontaneous combustion characteristics and hazards of the low-temperature oxidation (LTO) stage in the process of spontaneous combustion of coal and mudstone, the pore structure, spontaneous combustion characteristic parameters, and exothermic characteristics of coal and mudstone were tested and studied, and the oxidation kinetic parameters were calculated. The results show that mudstone has a larger specific surface area and pore volume than coal. From the fractal characteristics, the pore structure of mudstone is more complex than that of coal. According to the comparison of theoretical and actual gas generation and oxygen consumption rate curves, it is found that there is an interaction between coal and mudstone in the LTO process. With the increase of mudstone mass ratio, gas production, and its oxygen consumption rate increase. Among them, CM-4 (Coal:Mudstone = 1:1) has the highest exothermic intensity and the exothermic factor (A) and fire coefficient (K) increase with the increase of mudstone content. The apparent activation energy of the mudstone sample is lower than that of the raw coal, indicating that the sample after adding mudstone is more likely to have spontaneous combustion in the LTO stage.

Keywords Coal spontaneous combustion, Mudstone, Pore structure, Oxidation characteristics, Thermodynamic properties

Coal spontaneous combustion disaster in coal mine is not only a waste of resources but also a serious hazard to the health and safety of mine personnel¹⁻³. Coal self-ignition is a dynamic and complex physicochemical process. The heat accumulated by the LTO of coal is the power source of coal self-ignition⁴. The essence of self-ignition of coal is a complex oxidation kinetic process in which coal and oxygen undergo physical and chemical reactions and release a large amount of heat and carbon monoxide equal gas. Therefore, carbon monoxide can be considered to be an indicator gas, and the characteristic changes of the coal self-ignition process can be analyzed by using the indicator gas method combined with the oxidation kinetic equation. The index gas method⁵ refers to selecting the index gas and analyzing its relationship with temperature. Many researchers domestic and abroad have studied the index gas method and the characteristic parameters in the course of coal self-ignition. Deng⁶ studied the characteristics of coal with divergent metamorphic degrees in the course of LTO and self-ignition by the temperature-programmed experiment and oxidation kinetics analysis. It was found that the stronger the grade-crossing-elimination structure of metamorphism of the coal, the greater the feature temperature and activation energy, and the lower the likelihood of coal samples spontaneously igniting. Yan⁷ studied the impact of pre-oxidation on the LTO of coal, studied the exothermic and kinetic characteristics of the LTO reaction, and discussed the influence of oxidation temperature and oxygen volume fraction on activating the following LTO response of pre-oxidized coal. The results show that the LTO process of pre-oxidized coal lags behind that of raw coal. Ren et al.⁸ studied the risk of self-ignition of pulverized coal and measured the LTO heat flow of three kinds of metamorphic pulverized coal at different levels of oxygen concentration by the C80 microcalorimeter system. The results indicate that the decrease in the density of oxygen and the enhancement in the metamorphic extent of pulverized coal greatly reduced the risk index of self-ignition of pulverized coal.

¹College of Mining, Liaoning Technical University, FuxinLiaoning 123000, China. ²College of Safety Science and Engineering, Liaoning Technical University, FuxinLiaoning 123000, China. ³Institute of Safety Engineering and Technology, Liaoning Technical University, FuxinLiaoning 123000, China. ⁴College of Safety and Emergency Management Engineering, Taiyuan University of Technology, Taiyuan 030000, Shanxi, China. ✉email: Intuzjh@163.com

Zhang⁹ studied the variation of organic sulfur compounds in coal during LTO and found that the gas release during LTO of SO₂ is directly related to the metamorphic degree of coal and the content of the organic sulfur compound. Zhao¹⁰ studied the influence of water immersion on coal structure and LTO. It was found that the change in pore structure and the increase of free radical concentration caused by water soaking increased the possibility of contact among oxygen with active sites on the face of the pores, which made it more likely that the oxidation reaction would take place. Xiao¹¹ studied the influence of ionic liquids on the macroscopic construction and critical temperature of LTO coal samples and concluded that ionic liquids would lead to a reduction in oxidation reactivity and the deterioration of oxidation performance. Dai¹² studied the impact of oxygen supply on the LTO of coal and found that with the increase of oxygen concentration, the oxygen uptake rate and the yield of gaseous products increased to a certain extent. Zhong¹³ studied the heat effect of low-rank coal in the process of LTO after immersion in water and vacuum drying. It was found that the fast aliphatic chain-forming reaction was promoted after immersion in water and vacuum drying, which increased the initial heat release and made the coal more prone to self-ignition. Zhang¹⁴ studied the influence of long-term immersion in water on the LTO process of coal and concluded that long-term immersion led to significant periodic changes in the oxidation property of coal, of which 6 months of immersion time was crucial.

In the process of LTO of coal, lateral chain and various oxidized functional groups mainly participate in the reaction. The functional group is slowly activated and begins to react with oxygen. Among the many oxidized functional groups in coal, the hydroxyl group is the key active substance to induce the LTO of coal¹⁵, and the carbonyl group is considered to be helpful to induce the transformation of chemical adsorption to LTO¹⁶. Li et al.¹⁷ used a combination of LTO and low-temperature carbonization to determine the macro gas concentration of the two processes and then used in-situ infrared spectroscopy and in-situ EPR to determine the content of microscopic free radicals and oxygen-containing functional groups. It was discovered that low-temperature pyrolysis led to the degradation of oxidized functional groups and the creation of alkyl radicals. The thermal cracking of oxidized functional groups generates many active sites, which are oxidized at room temperature to release mass gas and release heat¹⁸. Meng¹⁹ studied the formation, release, and changes of active radicals of small molecular gases in low-rank coal during LTO by TG-DSC, TG-IR, and in-situ infrared measurements, and found that 100–200 °C is the key temperature for gas production. Zhang²⁰ studied the impact of radicals on heat during the influence of long-term immersion of bituminous coal was studied. The results showed that the hydroxyl content increased with the increase of the grade-crossing-elimination structure of metamorphism, and the key functional groups of bituminous coal played an important role in heat.

Coal inevitably undergoes various changes in its physical structure and surface morphology during LTO²¹, which affects the heat and mass transfer efficiency when oxidizing coal at low temperatures²². To illustrate, the micropores of the coal affect the maximum heat release and the initial heat release of LTO²³. During the LTO of coal, many mesoporous channels are formed. These provide a physical space for oxygen migration and adsorption²⁴. In the process of LTO, in general, the amount of oxygen adsorbed on the coal surface is affected by the growth of the pore structure. Cai et al.²⁵ studied the surface physical microstructure evolution of different metamorphic coals during LTO and explained the influence of coal surface texture on oxidizing property through pore connectivity and oxygen adsorption on coal surface during coal oxygen reaction.

At present, the research on low-temperature oxidation (LTO) of coal has been relatively perfect, but the research on LTO of mudstone and coal blending is relatively scarce. In fact, in the process of coal mining, the roof mudstone will collapse and mix with coal in the goaf. Therefore, in this paper, the temperature-programmed experiment and low-temperature nitrogen adsorption experiment were used to test the LTO process of coal-rock mixtures with different mass ratios. The specific surface area, pore volume, pore size distribution, and fractal characteristics of coal and mudstone were compared, and the changes in index gas, oxygen consumption rate, exothermic intensity, oxidation kinetic parameters, and other parameters in the LTO process of coal and mudstone were discussed. The research results are of great significance to the spontaneous combustion characteristics of the coal-rock mixture in an LTO process in Goaf.

Materials and methods

Samples preparation

The test coal samples were taken from Pingzhuang lignite in Inner Mongolia, and the rock samples were taken from the mudstone of the coal seam roof. After sampling, it was sealed under a vacuum and taken to the laboratory. The lignite and mudstone were ground to 100–150 mesh with a jaw crusher. The coal sample and the rock sample were mixed according to the mass percentage ratio of 1:0, 1:0.1, 1:0.4, 1:0.7, 1:1 and 0:1, Named C, CM-1, CM-2, CM-3, CM-4, M, vacuum drying at room temperature for 24 h, sealed and stored. The industrial analysis of coal and mudstone is shown in Table 1.

Sample	M _t /%	A _{ad} /%	V _{ad} /%	FC _{ad} /%
Coal	9.17	12.37	32.91	45.55
Mudstone	2.79	87.33	8.25	1.63

Table 1. Proximate analysis of coal and mudstone.

Experiments

Specific surface determination

The pore distribution of coal and mudstone samples was measured by BELSORP-maxII specific surface area and pore size distribution analyzer of Macchibay, Japan. The test sample mass is approximately 1 g. This was followed by the calculation of specific surface area and pore distribution using BET multilayer adsorption theory and BJH.

Temperature programmed gas production experiment

The ZRD-II coal spontaneous combustion characteristic tester and HW-2000 chromatograph combined system were used to take 10 g coal-rock mixed samples. The mixed coal sample was placed in a coal sample tank for a temperature rise test. Fresh air (oxygen volume fraction of 20.95%) was introduced, the flow rate was 30 mL/min, and the temperature was increased from 40 to 200 °C. When the coal temperature reached the temperature point to be measured, the air pump was opened to pass the gas into the chromatograph, and the gas analysis and recording were completed in the computer terminal software. The experimental equipment and steps are shown in Fig. 1.

Results and discussions

Pore structure analysis

Low temperature N₂ adsorption test results

Figure 2 shows the low-temperature N₂ adsorption/desorption isotherms of coal and mudstone. The N₂ adsorption/desorption isotherms show a significant hysteresis loop in the range of P/P_0 between 0.45 and 1 and are classified as type IV or IV (a), which is strongly linked to the capillary condensation in the mesopores²⁶. At about $P/P_0 = 0.5$ the steep region of the desorption isotherm leads to the lower closing point of the hysteresis loop. Monolayer and multilayer adsorption, dominated by van der Waals forces, produces the initial part before the lower closure point²⁷. The hysteresis curve of coal and mudstone belongs to the H3 type, representing slit-like pores²⁸, indicating that the pores are in a half-open position. Compared with coal, mudstone has a more obvious hysteresis loop. The more apparent the hysteresis effect, the worse the pore network connectivity, which also suggests that there are a large number of irregular nanopores in mudstone. It is worth noting that when the relative pressure is 0.5, there is a mutation point in the desorption branch, which represents the minimum value of pore development²⁹. The amount of nitrogen adsorbed in the studied samples varies greatly, while mudstone adsorbs more nitrogen at the highest relative pressure (about 22.078 cm³/g), showing greater adsorption capacity, while coal adsorbs less nitrogen (about 3.695 cm³/g). According to the characteristics of the adsorption, the isothermal adsorption curve can be partitioned into three stages, stage I ($P/P_0 < 0.1$), stage II ($P/P_0 = 0.1-0.8$) and stage III ($P/P_0 = 0.8-1$). The first stage is the low-pressure stage. The gas adsorption in this stage mainly exists in the form of single-layer adsorption. Due to the low micropore content, the adsorption capacity of coal and mudstone is low, and the adsorption curve rises slowly. With the increase of relative pressure, the adsorption of a single layer is completed. Entering the intermediate pressure stage, the power-level trip of adsorption of coal and mudstone increases with the increase of relative static pressure, but the rate of increase of the two is different. The power-level trip of adsorption of coal began to augment when the relative static pressure reached about 0.6, while the power-level trip of adsorption of mudstone continued to increase during the medium pressure process. Within this relative pressure enclosure, with the increase of relative static pressure, the adsorption of N₂ in coal pores moderately changes from single-layer adsorption to polymolecular layer adsorption on larger borehole wall (Pores capable of accommodating at least two layers of nitrogen). If the relationship between relative pressure and pore width satisfies the Kelvin equation, capillary condensation occurs in the pores³⁰. With the increase of pressure, the N₂ molecule will undergo agglomeration in larger pores. The third stage is the high-pressure stage,

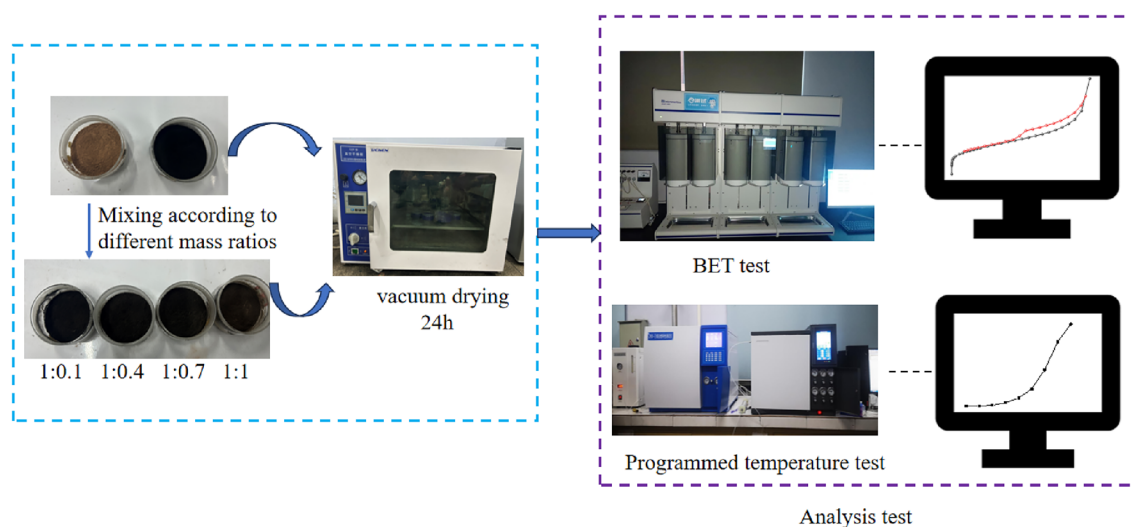


Figure 1. Flow chart of experiment.

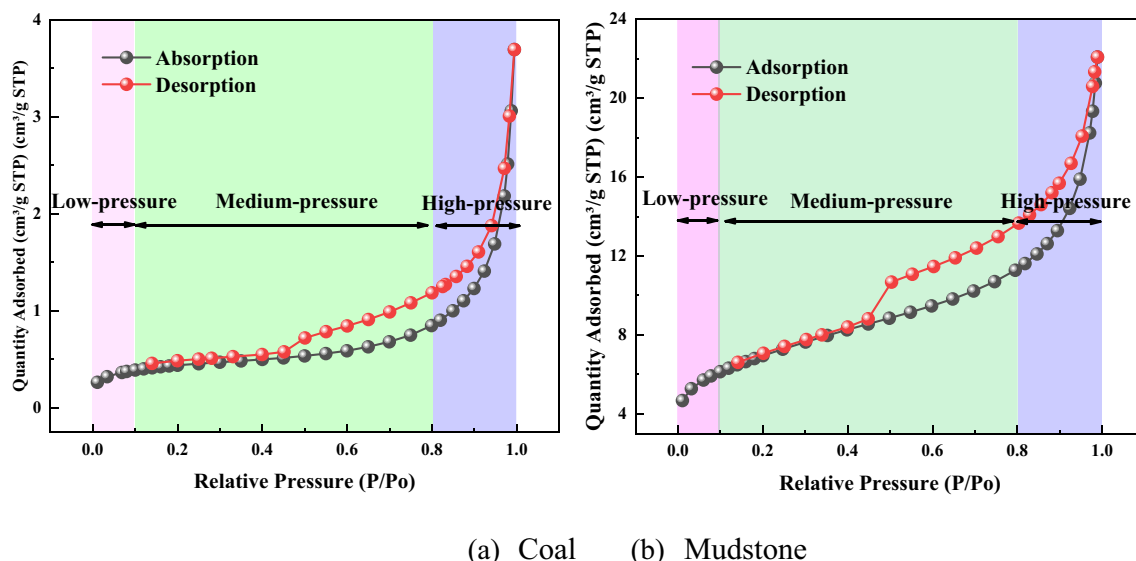


Figure 2. Adsorption/desorption curves of lignite and mudstone. (a) Coal. (b) Mudstone.

and the sorptive capacity of coal and mudstone increases exponentially in this area. This indicates that there is massive liquefaction of N_2 in the macro pores or on the faces of the sample³¹, resulting in a dramatic increase in N_2 sorptive ability. Even at relative pressures near 1, there is still no attachment threshold. Pay attention, the sorptive capacity of mudstone has kept a greater growth rate throughout the process. This suggests that there are pores of appropriate size at any relative pressure band. Therefore, the pore distribution of mudstone is more homogeneous than that of coal samples. This means that the adsorption ability of the sample is superior to that of the coal used.

Pore structure evolution

Table 2 gives the pore structure parameters of coal and mudstone. It can be seen that the specific surface area of mudstone is 21.18 times that of coal. Mudstone has a larger specific surface area than coal, so mudstone can adsorb more gas. The total pore volume of mudstone is 5.98 times that of coal, signifying that the porous micro-structure of mudstone is more developed, with more mesopores and macropores.

Density functional theory was used to analyze the adsorption isotherm curves of coal samples, and the pore size distribution of coal samples in the range of 0–30 nm was obtained. The red curve in Fig. 3 reflects the variation in cumulative pore volume, and the black curve shows the variation rate of increase of pore space volume with pore size. The broad peak indicates that the pore size of the interval in question is a complex one, and the narrower peak means that the pore size of the interval is fairly uniform. See Fig. 3, when the pore size is under 2 nm, the v , and dv of the coal sample are close to 0, indicating that it contains a small amount of micropores. There is a strong peak at 2–5 nm in both coal and mudstone, signifying that there are more pores in the range of 2–5 nm, and the pore size is concentrated at about 4.2 nm. In the range of 5–30 nm, there are many peaks of different sizes, indicating that coal and mudstone distribute many pores with uneven pore size in this range.

The BJH method was used to examine the adsorption isotherms, and the pore volume and pore percentage in the range of 0–150 nm were obtained. It can be seen from Fig. 4 that the pore volume of coal and mudstone is mainly provided by mesopores, accounting for 53.6% and 76.08% of the total pore volume, respectively, followed by macropores, accounting for 44.8% and 20.71% of the total pore volume, respectively, and micropores account for the least. Within the pore volume of 30 nm, the pore volume at 2–5 nm accounts for the largest proportion, which corresponds to the strong peak at 2–5 nm in Fig. 3.

Fractal dimension calculation

The fractal dimension (D_s)^{29,32} is widely used to represent the surface complexity and smoothness of holes. Studies have shown that in the process of adsorption, desorption, and diffusion, an important role is played by the irregularity of the pore surface. The Frenkel–Halsey–Hill (FHH) model was used to analyze the N_2 isothermal adsorption/desorption process of coal. Compared to other models, the FHH model is the most effective³³.

Coal sample	Specific surface area (m^2/g)	Total pore volume (cm^3/g)	Average pore size (nm)
M	1.16118	0.005715	14.1829
Y	24.9520	0.034151	5.4746

Table 2. Specific surface area and pore structure parameters of coal and mudstone.

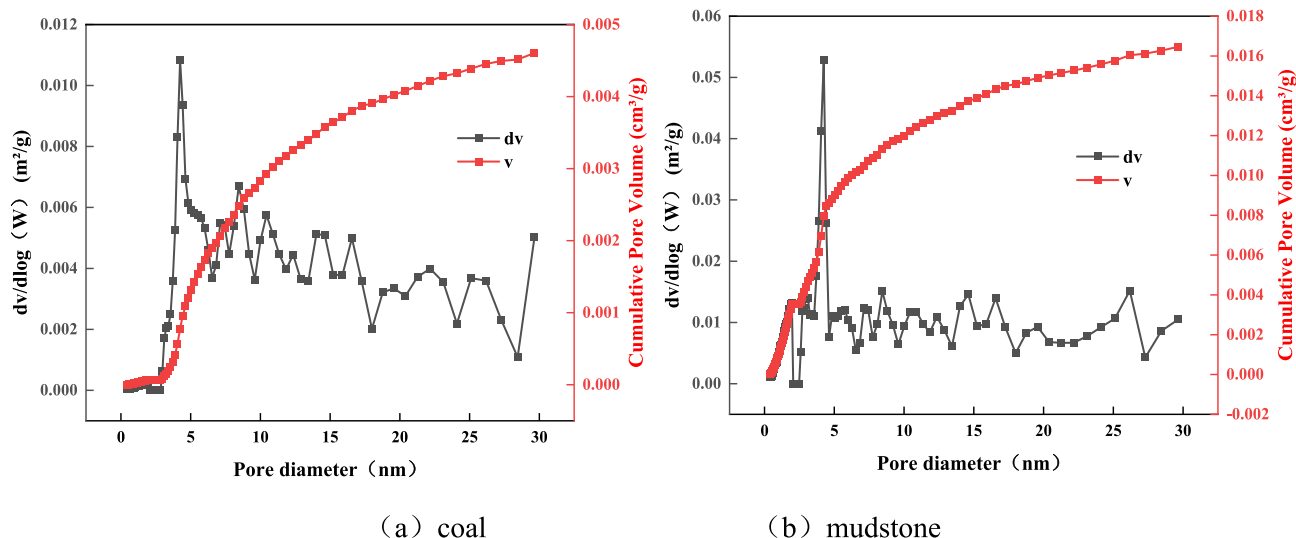


Figure 3. PSDs of coal and mudstone (pore size less than 30 nm). (a) Coal. (b) Mudstone.

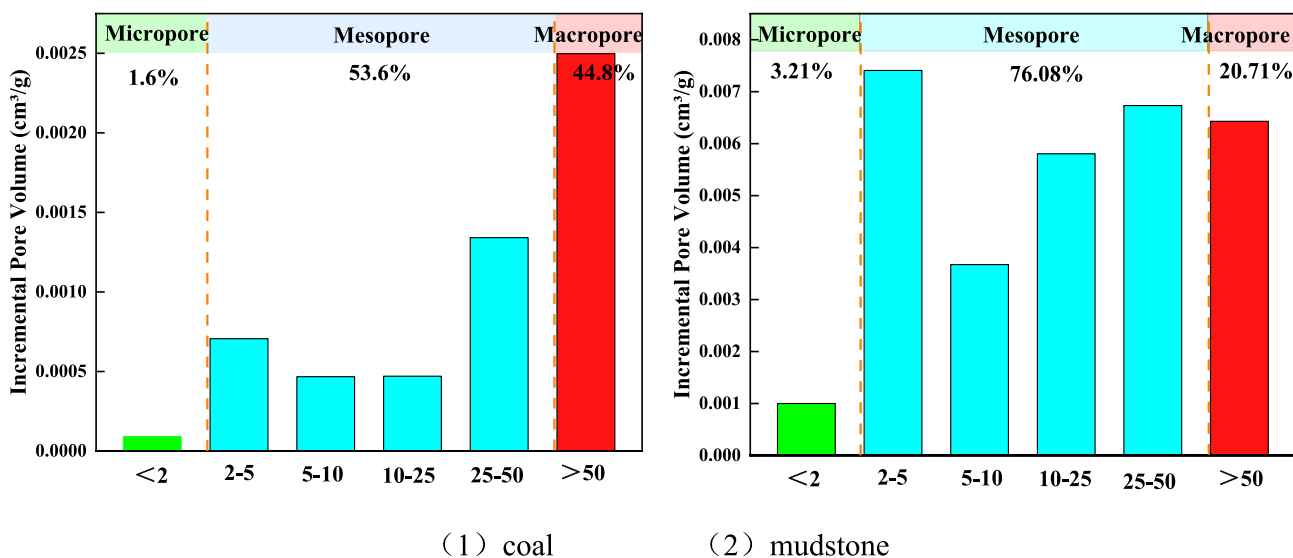


Figure 4. Coal and mudstone pore volume increment. (1) Coal. (2) Mudstone.

Based on the data from the gas adsorption diagram, the FHH diagram can be generated (see Fig. 5). As a general rule, the FHH curve has a closure point at $P/P_0 = 0.5$. The curve is split into two parts, and the fractal number of dimension D_s of the two parts is denoted by D_1 and D_2 , respectively. D_1 is the surface roughness characterization of pores, and D_2 is a characterization of the complexity of the pore structure. The higher the D_1 value, the coarser the surface of the pores; the higher the D_2 value, the more complex the structure of the pores. As shown in Fig. 5, the fractal characteristics of mudstone and coal, in which the greater the coefficient of association R^2 , the more meaningful the fractal properties. It can be seen from Fig. 6 that the D_1 of coal and mudstone is the same, indicating that the roughness of the pore surface of the two is similar, but the D_2 of the two is very different. The D_2 of mudstone is 0.20594 greater than coal, signifying that the pore structure of mudstone is more complex than that of coal, which is reflected in the pore size distribution of Fig. 3. The fractal dimension of mudstone samples is greater than 2.6, indicating that the surface roughness is high, the pore connectivity is poor, and the reservoir heterogeneity is strong³⁴. Among them, mudstone $D_2 > D_1$, reflecting the heterogeneity of mudstone pore structure is slightly stronger than pore surface roughness and micropore irregularity. Studies have shown that³⁵, when the complexity of the pore structure of macropores is greater than that of micropores, D_2 will be greater than D_1 . The reason is that the types of macropores are diverse, including intergranular pores, intragranular pores, intercrystalline pores, etc., while the types of micropores are relatively simple, so the macropore structure is more complex. It has a fairly loose spatial structure, which is similar to the study of Zhao et al.³⁶. The coal $D_1 > D_2$ indicates that the irregularities and disturbances of the coal surface are more sturdy than the irregularity and disorder of the pore structure inside the coal. Similar to adsorption performance and pore structure properties.

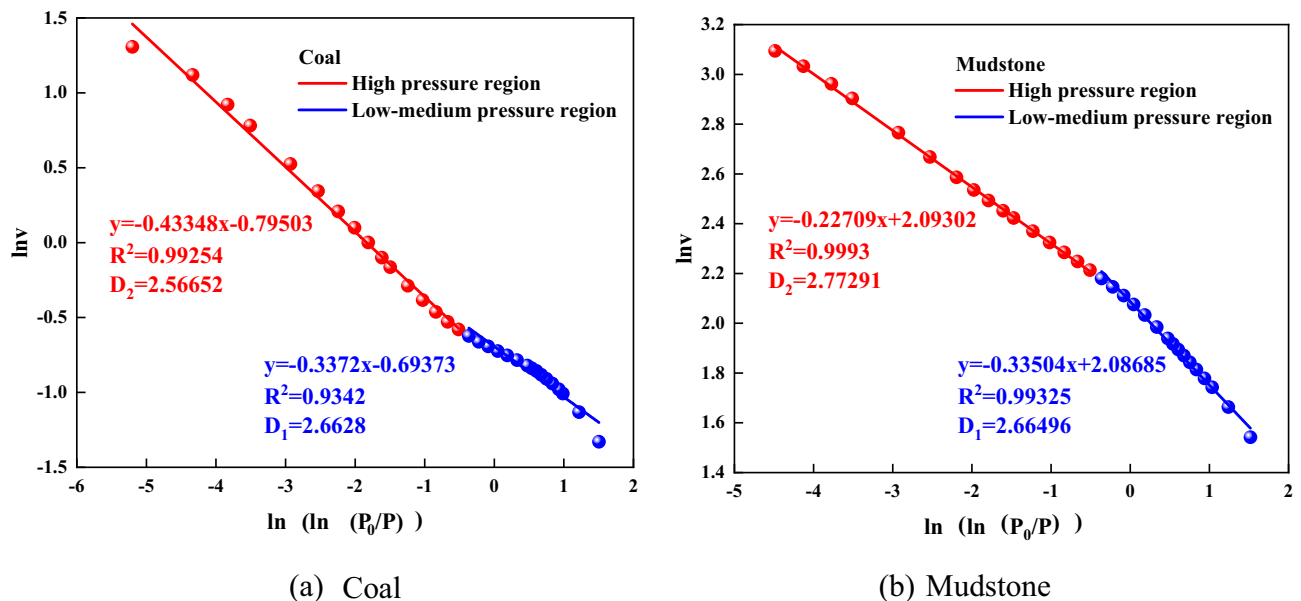


Figure 5. FHH model calculation results. (a) Coal. (b) Mudstone.

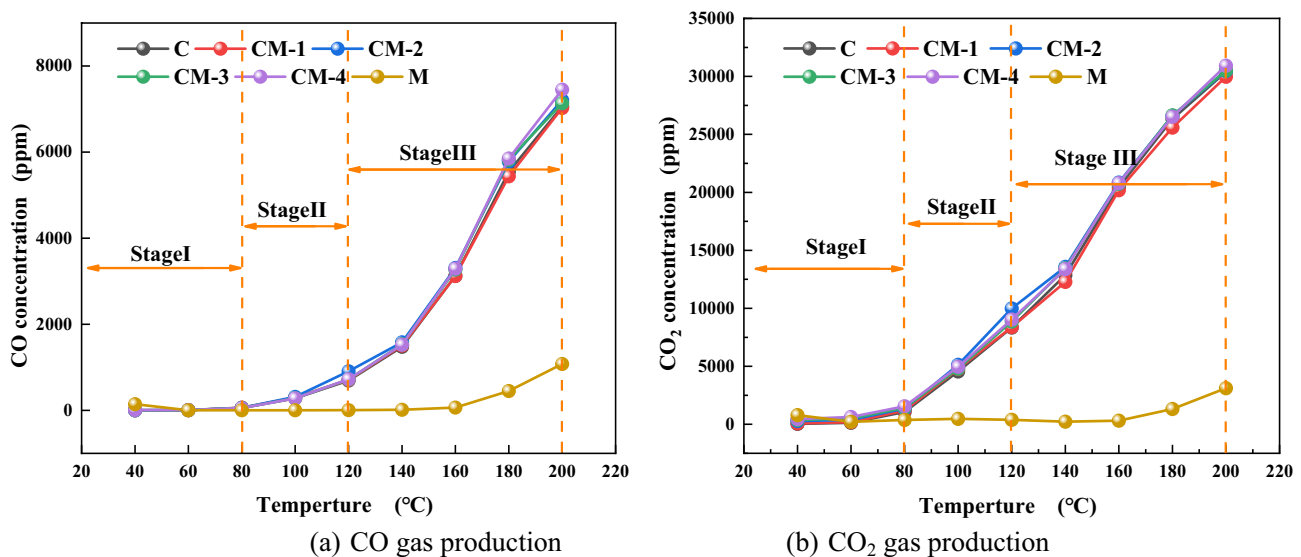


Figure 6. Analysis of CO and CO₂ production of coal and mudstone and coal-rock mixtures with different mass ratios. (a) CO gas production. (b) CO₂ gas production.

In summary, coal and mudstone are complex porous materials, and these pores affect adsorption, desorption, diffusion, and seepage. The pore size, pore volume, and specific surface area of coal and mudstone affect their oxygen absorption capacity, which in turn affects the spontaneous combustion characteristics of coal.

Experimental analysis of temperature programming

Analysis of ionic gas production

Coal spontaneous combustion is a slow process, the oxidation process will produce different gas products, such as carbon monoxide, carbon dioxide, and other gases. Carbon monoxide gas is the main product of the photooxidation reaction of coal. In contrast to other gaseous products, CO gas is produced when coal begins to spontaneously combust, which bodes well for spontaneous coal burning.

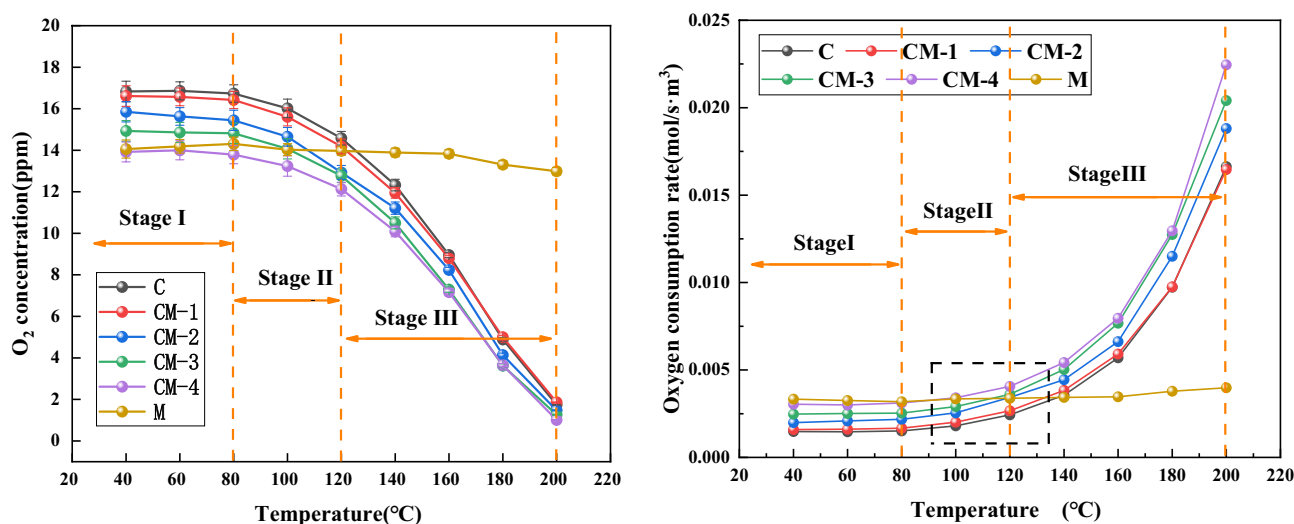
Figure 6a shows the variation of carbon monoxide and carbon dioxide production with temperature in coal-mudstone and coal-rock mixtures with different proportions, while Fig. 6b shows the trend in CO₂ production with temperature. According to the data analysis, the changing trend of CO₂ and CO curves of coal and coal-rock mixture is consistent. In the LTO stage, the production of carbon monoxide, and carbon dioxide is gradually increasing, showing an exponential growth trend. According to the gas growth trend, the oxidation at the ambient temperature curve is divided into three stages, and the specific division details are given in the figure. In the

first stage, because the temperature is not fully accumulated, the CO yield of the sample remains unchanged, so the oxidation reaction remains slow. However, a small amount of CO and CO₂ gas is released from mudstone before 60 °C. The reason is that the specific surface area of mudstone is larger than that of coal, and the secondary CO in the free state of pores begins to desorb³⁷, this leads to relatively high CO and CO₂ production at this stage. As temperature rises, entering the second stage, the active groups on the surface of coal begin to chemically adsorb and the active sites generated during the heating process begin to react with oxygen to produce CO, which makes the CO generation of coal and samples added with mudstone began to increase. At this stage, the gas production of mudstone showed a steady trend. At this stage, the mudstone had insufficient aromatic and aliphatic compounds³⁸. As a result, it will not undergo an oxidation reaction in this process. In the third stage, the reaction between the coal and the oxygen is very intense, and the CO and CO₂ gases increase exponentially and enter the rapid oxidation stage. The CO and CO₂ production of mudstone begins to increase slightly after 160 °C, and the low content of carbon is oxidized in this process. The chemical adsorption of mudstone begins to produce a small amount of CO and CO₂ gases.

In summary, during the LTO process of coal-rock mixtures with different mass ratios, the gas production curve is similar to raw coal. The CO and CO₂ gas concentrations of coal-rock mixtures are more than those of raw coal and mudstone, but the increase is not large. It shows that there is a certain interaction between mudstone and LTO of coal.

Oxygen consumption rate analysis

The theory of coal-oxygen reaction has revealed the microscopic mechanism of coal oxidation^{41,42}. Oxygen is the dominant factor of the coal-oxygen response. Figure 7 is the comparison of oxygen consumption rates of coal-rock mixtures with alternative mass ratios and coal and mudstone. The oxygen concentrations of coal and mudstone and coal-rock mixtures with different mass ratios are shown in Fig. 8a. The oxygen concentration gradually decreases as the temperature increases, as can be seen from the figure, and the decrease is more evident with the rise of mudstone content. See Fig. 8b, in stage I, due to the low level of coal oxidation, the variation in oxygen consumption rate is not obvious, and the corresponding oxygen consumption rate³⁹ is low. The samples of coal and mudstone are consumed in a small amount of oxygen in the first stage. At this point, physical adsorption is the main controlling factor of the coal-oxygen responses. The intensity of the physical adsorption reaction is relatively weak, resulting in a gentle increase in the standard oxygen consumption of coal. At this time, there is a large amount of oxygen consumption in mudstone and the consumption remains stable in the first stage. The reason is that mudstone has a large specific surface area and a relatively developed pore structure, and a large amount of oxygen is adsorbed during this period. As coal temperature increases, the number of reactive functional groups and active sites increases, especially in stage II and stage III, the highly absorbent substances in mudstone promote the vaporization of coal water⁴⁰, more active sites begin to be exposed, and the rate of oxidation of the coal is accelerated, which in turn accelerates the oxygen consumption velocity. As the volume of mudstone added increases, the oxygen demand rate of the sample increases, indicating that the addition of mudstone accelerates the chemical oxygen of the mixed sample. The chemical oxygen rate of all samples except mudstone shows an upward trend. Through industrial analysis, it is possible to see that the lower carbon content and its lower volatile matter in mudstone are related to its difficult oxidation reaction⁴¹.



(a) Comparison of oxygen concentration (b) Comparison of oxygen consumption rate

Figure 7. Comparison of oxygen concentration and oxygen consumption rate of coal and mudstone and coal-rock mixtures with different mass ratios. (a) Comparison of oxygen concentration. (b) Comparison of oxygen consumption rate.

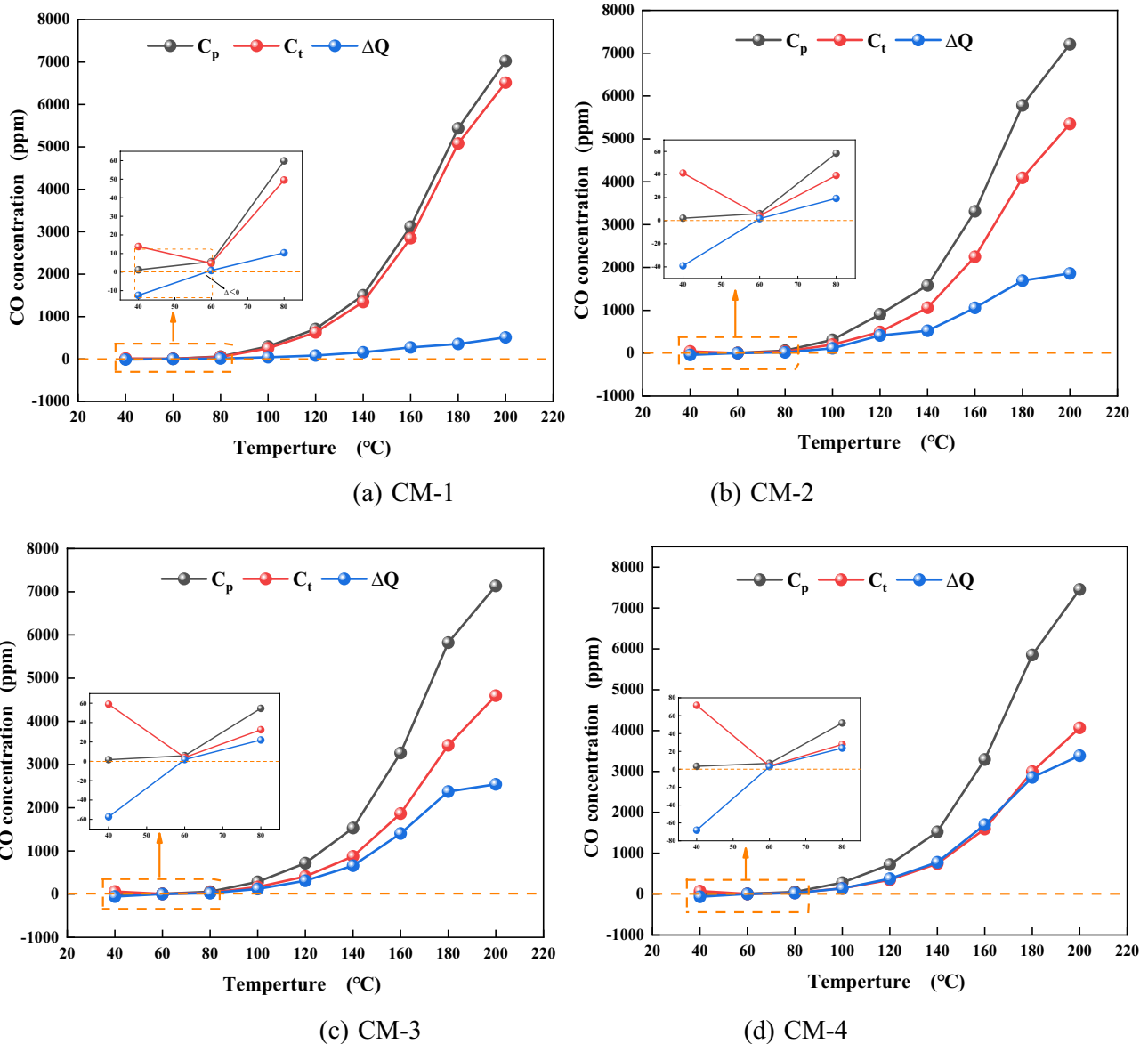


Figure 8. Changes of actual CO production and theoretical CO production during LTO of coal-rock mixtures with different proportions. (a) CM-1. (b) CM-2. (c) CM-3. (d) CM-4.

Transactional analysis

To investigate the mechanism of mudstone and coal in the ambient temperature oxidation stage, the experimental study of coal and mudstone was carried out. The theoretical gas production curve C_t and the theoretical oxygen demand rate curve O_t of the coal and mudstone mixture were calculated by the equation model. The difference between the gas production curve ΔQ and the difference between the oxygen consumption rate curve ΔH were calculated by the equation. The calculation method is shown in Eqs. (1)–(4):

$$C_t = x_m C_m + x_y C_y \tag{1}$$

$$O_t = x_m O_m + x_y O_y \tag{2}$$

$$\Delta Q = C_p - C_t \tag{3}$$

$$\Delta H = O_p - O_t \tag{4}$$

where x_m, x_y is the mass fraction of coal and mudstone, %; C_m, C_y is CO gas release from coal and mudstone, ppm; O_m, O_y is oxygen consumption rate of coal and mudstone, %.

The changes of ΔQ and ΔH in the course of LTO of coal and mudstone under different mass ratios are compared as shown in Figs. 8 and 9. The results show that mudstone samples with different mass ratios have some

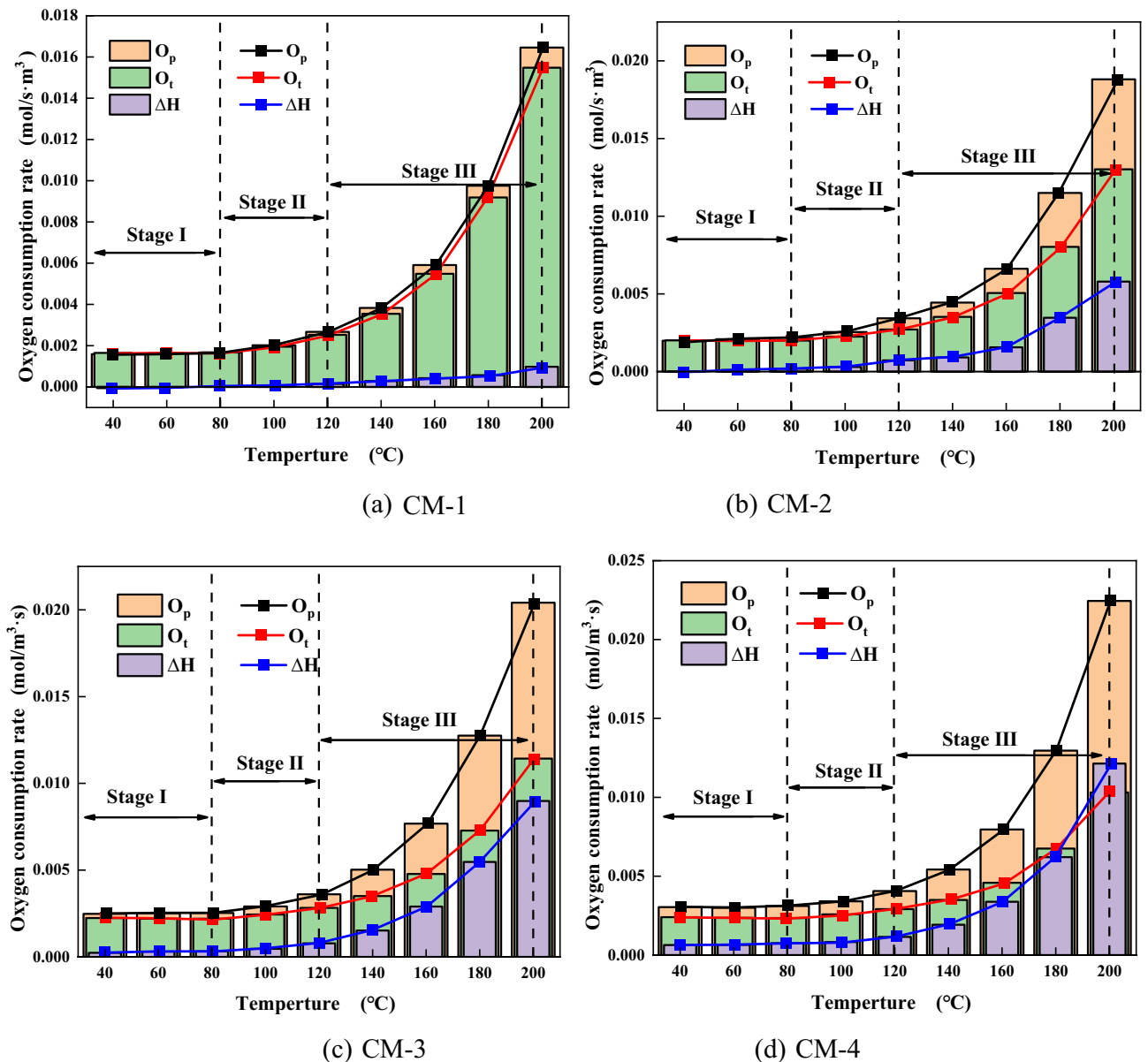


Figure 9. Changes of actual oxygen consumption rate and theoretical oxygen consumption rate during LTO of coal-rock mixtures with different proportions. (a) CM-1. (b) CM-2. (c) CM-3. (d) CM-4.

impact on the interaction in the process of LTO. It is visible from Fig. 8a that when the temperature is less than 60 $^{\circ}\text{C}$, $\Delta Q < 0$, there is a mutual inhibition effect between coal with rock at this stage. The strong absorbent minerals illite and montmorillonite in mudstone absorb the water in coal⁴². The free water is covered on the surface of the sample and enters the pores, which hinders the gas desorption of the sample so that the actual gas release of the mixed sample is lower than the theoretical gas release at this stage. At 60–200 $^{\circ}\text{C}$, ΔQ and ΔH are greater than 0. It can be seen from the variation of ΔQ and ΔH of each sample in Fig. 10 that ΔQ and ΔH gradually rise with the increase in silt content, indicating that there is a mutual promotion effect between mudstone and coal at this stage, and the greater the mudstone content is, the more pronounced the promotional impact. The reason is that the higher sulfur content and mineral content in mudstone plays a catalytic part in the oxidation reaction of the sample⁴³. The additive of mudstone accelerates the oxygen consumption of the mixed sample. The larger specific surface area of mudstone adsorbs a large amount of oxygen. The more mudstone provides more adsorbed oxygen, which provides an oxygen supply channel for coal oxidation. The oxygen consumption increases significantly, the functional groups in coal are further active, and active sites are continuously generated⁴⁴. A steady stream of oxygen molecules is adsorbed on these active sites, resulting in an increase in CO and CO₂ gas production. It shows that in the procedure for LTO, mudstone has played a certain role in promoting coal spontaneous combustion.

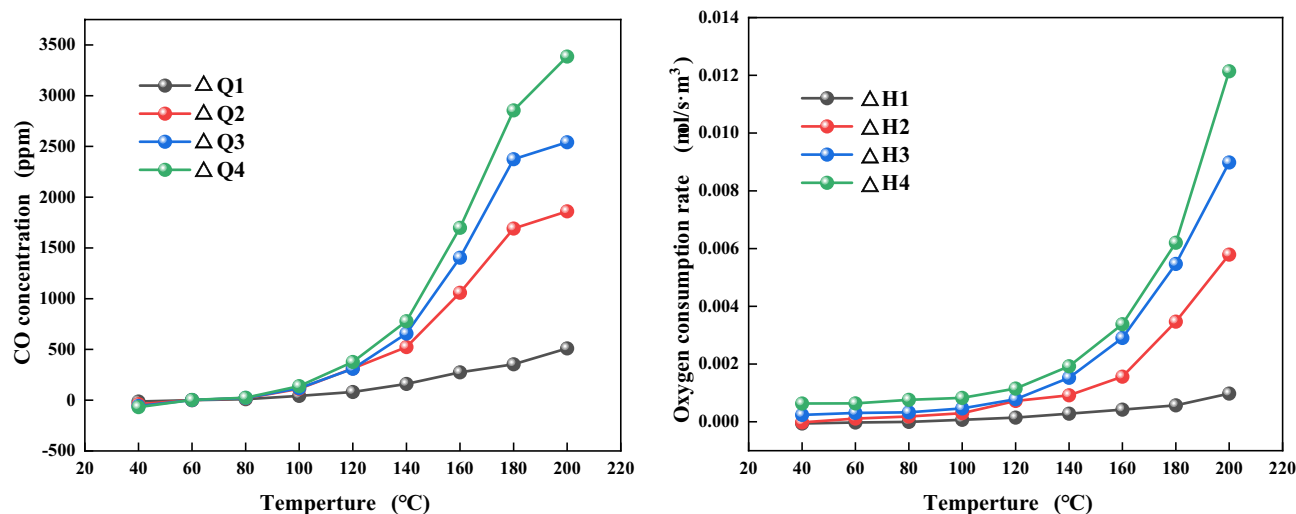


Figure 10. Changes of ΔQ and ΔH of each sample.

Analysis of heat release intensity

Exothermicity

Coal spontaneous combustion is a phenomenon caused by the continuous rise of coal temperature due to the photooxidation reaction of coal with oxygen in the air and the release of a huge quantity of reaction heat. Therefore, in the combustion of coal, the exothermicity of coal can characterize the oxidation process of coal at a certain temperature point or a certain temperature range. As an important index to measure the heat release of coal, the calculation and analysis of heat release intensity is indispensable. According to the change of bond energy, the calculation formula of exothermic intensity is estimated. See Eq. (5):

$$q_{\max}(T) = \Delta H_{20}[v_{O_2}(T) - v_{CO}(T) - v_{CO_2}(T)] + \Delta H_{CO}v_{CO}(T) + \Delta H_{CO_2}v_{CO_2}(T) \quad (5)$$

where, q_{\max} is the maximum exothermic intensity, $J/(cm^3 s)$; T is the thermal temperature of coal, K; ΔH_{20} is the average heat of the second step, 284.97 kJ/mol; v_{O_2} is oxygen consumption rate, $mol/(cm^3 s)$; v_{CO} is the CO production rate, $mol/(cm^3 s)$; v_{CO_2} is the rate of CO_2 production, $mol/(cm^3 s)$; the average reaction heat of ΔH_{CO} to 1 mol CO, 311.9 kJ/mol; ΔH_{CO_2} is the average reaction heat of generating 1 mol CO_2 , which is 466.7 kJ/mol.

It can be seen from Fig. 11 that the exothermic intensity of coal and coal-rock mixtures with different proportions increases with the temperature rise. In the three stages of LTO, the oxidation reaction intensity of the samples is different. In stage I, only a small quantity of easily oxidized primary active groups participate in the reaction, create secondary groups of active users, and release a small amount of heat. At this time, the addition of mudstone has only a minor impact on the heat release of the sample. In stage II and stage III, with the rise of mudstone content, the heat release intensity shows an increasing trend. The highest intensity of the thermal output of CM-4 is $4533.9 \times 10^5 (J cm^{-3} s^{-1})$, which is 1.33 times that of raw coal. On the one hand, mudstone

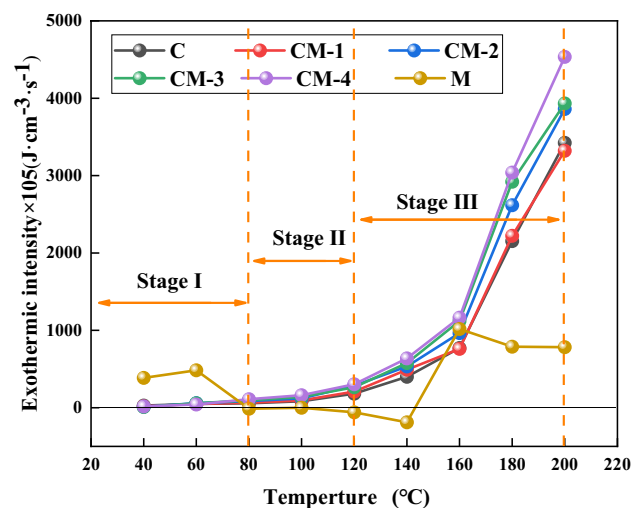


Figure 11. Comparison of heat release intensity.

provides sufficient oxygen channels for coal oxidation, the active groups in coal are also activated, and the secondary groups of active users continue to oxidize, thus the release of a large amount of heat. On the other hand, the thermal diffusivity and the thermal conductivity of the sample can be improved by the addition of mudstone, Lower its specific heat content, and support of thermal exchange of the coal sample⁴⁰. The mudstone shows irregular heat absorption and release during the whole process.

Exothermic factor

The heat production of coal needs oxygen uptake, and the heat generation and oxygen uptake of the coal body lead to the oxygen partial in circumstances lower than that in the air. In the process of coal oxidation heating, the intensity of oxidation heat release is dominant, which is inextricably linked to the rate at which oxygen is consumed. Yan⁴⁵ has studied the connection between the rate of oxygen uptake with the intensity of heat release of coal and has found that the exothermicity of coal is proportional to the rate of oxygen uptake, which can be expressed as:

$$HF = Av_{O_2} \quad (6)$$

where A is defined as the exothermic factor, HF is the exothermic intensity of each sample, and v_{O_2} is the oxygen uptake rate of each sample.

The information from the exothermic intensity and oxygen uptake rate achieved by the fitting experiment of Eq. (6), is used to determine the relationship between the O_2 consumed and the exothermic intensity at different oxidizing concentrations, see Fig. 12, and the fitting results in Fig. 12 are further counted, as shown in Table 3. The exothermic factor A of the samples added with mudstone increased by 0.01752–0.11185 relative to raw coal. The exothermic factor increased with the addition of more mudstone, and the two showed a linear relationship. It shows that the oxidation reaction of the sample after adding mudstone is more sensitive to the concentration of oxygen. The oxidation reaction rate of coal depends on the contact area between coal and oxygen to a certain extent. The addition of mudstone makes the specific surface area of the whole sample larger, the greater the surface area of contact between the dioxygen molecule and the carbon molecules, the more contact there is, and eventually the more severe the oxidation reaction. The exothermic factor A can be used as an index for the assessment of the severity of the oxidation effect of the self-ignition of coal samples. The exothermic factor of samples after adding mudstone is more than that of raw coal, implying that the risk of spontaneous combustion increases after adding mudstone.

Greenham fire coefficient

Graham observed that the gas produced after oxidation is related to adsorbed oxygen, and by comparing the rate at which CO is produced with the rate at which O_2 is consumed, an index was established to calculate the level of heating^{46,47}, which is still the most effective tool for detecting and evaluating underground fires in coal mines. This ratio is used to measure the oxidation strength of coal. In case of low temperatures, coal is oxidized to produce a small amount of carbon monoxide, while consuming a lot of oxygen. When the temperature rises, increasing amounts of oxygen are converted into carbon monoxide, so the ratio of the produced carbon monoxide to the removed or depleted oxygen will show strength. The defined fire coefficient is shown in Eq. (7):

$$k = \frac{\Delta CO}{\Delta O_2} \times 100\% \quad (7)$$

Figure 13 shows the variation of fire coefficient with temperature. It can be seen that the fire coefficient has a slight upward trend in stage one, but does not exceed the safety line. In the second stage, the change point begins to appear at about 100 °C. CM-4, CM-3, CM-2, CM-1, and C exceed the safety line in turn. At this time, active groups in coal and their high-energy compounds are destroyed, reacting with oxygen to release large amounts of gas. In stage III, with the increase of the addition amount, the critical line of 40% is exceeded, the temperature rises rapidly, reaches the ignition temperature quickly, reaches the peak at 180 °C, and the peak of CM-4 is up to 161%. It shows that the addition of mudstone makes the rate of increase of CO concentration and the rate of decrease of oxygen concentration change significantly, which accelerates the oxidation reaction, and the higher the mudstone content, the more obvious the oxidation acceleration effect.

Activation energy analysis

According to the research of Zhong et al.^{48,49}, the calculation formula of activation energy is shown in Eq. (8).

$$\ln c_{out} = -\frac{E}{RT_i} + \ln(ASLmc_{O_2}^n/kv_g) \quad (8)$$

where, L is the length of the coal sample tank, m ; c_{out} is the CO concentration at the outlet of the coal sample tank. S is the cross-sectional area of the coal sample container, m^2 ; k is the Unit Conversion Coefficient used to convert, 22.4×10^9 ; v_g is the air-flow rate, m^3/s ; T_i is the absolute temperature of coal, K ; A is the pre-exponential factor; $c_{O_2}^n$ is the he content of oxygen in the reaction gas, mol/m^3 ; n is the order of reaction; E is the energy-dissipating pile of activation, J/mol ; R is the molar gas constant, $8.314 J/(mol K)$.

It can be seen from Eq. (8) that there is a linear relationship between $\ln c_{out}$ and $1/T$ when the ventilation flow rate is constant, and the equivalent activity of various stages of the coal-oxygen reaction can be obtained by computing the gradient. The LTO is divided into two processes. Before 120 °C, it belongs to the slow accelerated oxidation process, and after 120 °C, it belongs to the rapid oxidation process. The fitting calculation results are shown in Fig. 14. The changing trend of raw coal and mudstone samples in the whole LTO stage is the same,

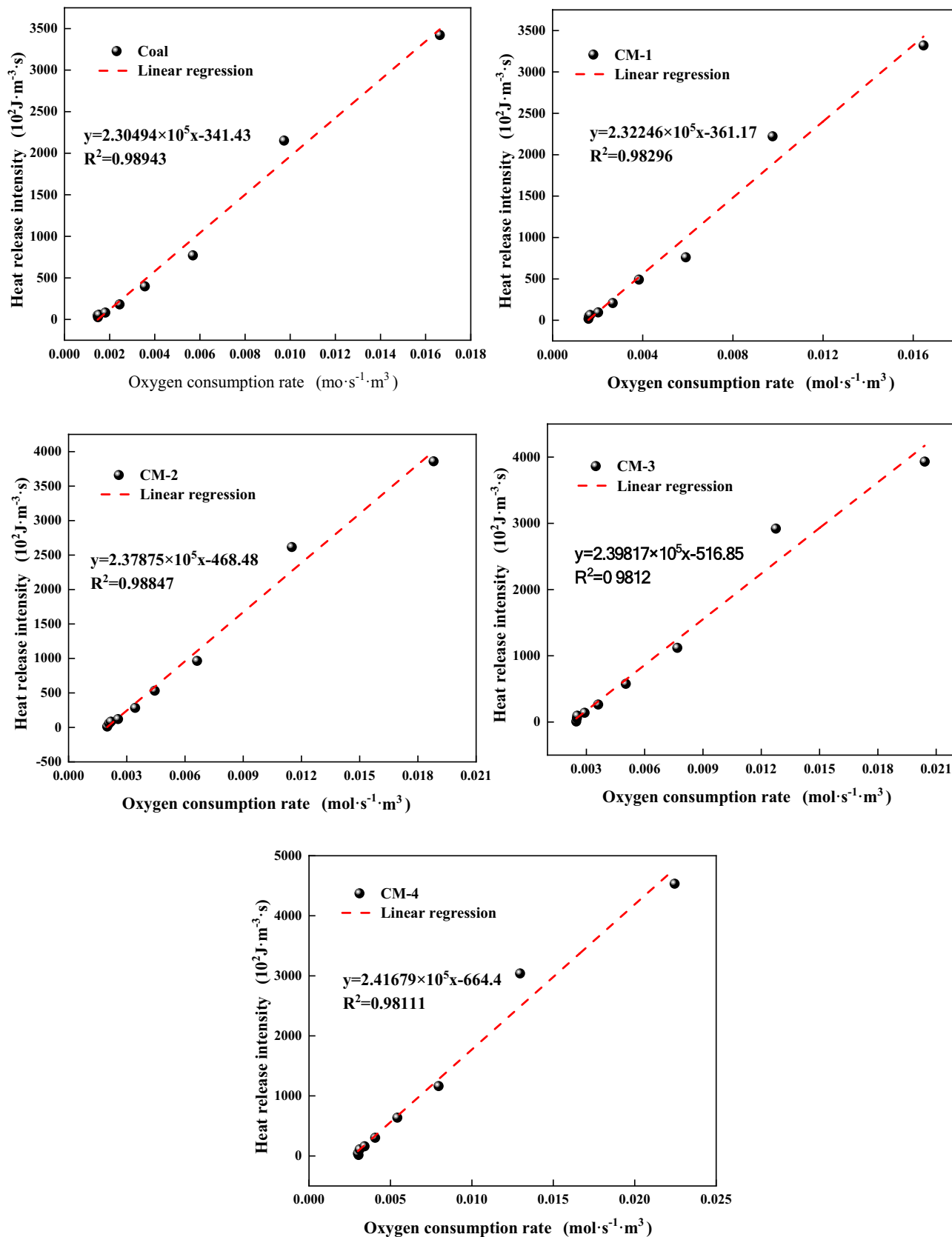


Figure 12. Fitting curve of exothermic factor.

Sample	A	R ²
M	2.30494	0.98943
CM-1	2.32246	0.98296
CM-2	2.37875	0.98847
CM-3	2.39817	0.9812
CM-4	2.41679	0.98111

Table 3. Comparison of exothermic factors of each sample.

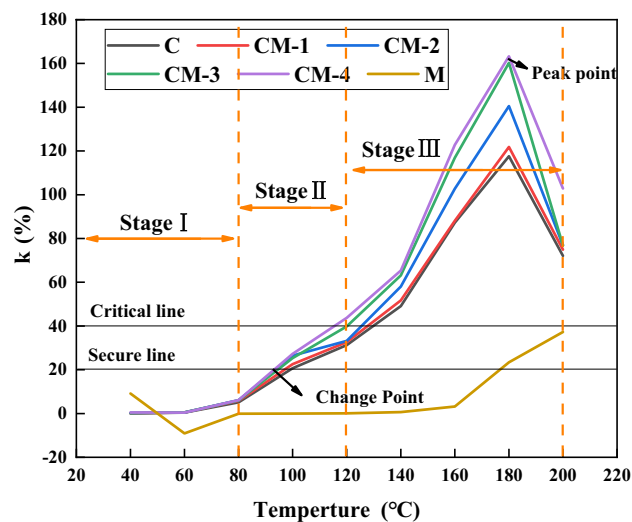


Figure 13. Variation of fire coefficient of each sample.

and the energy-dissipating pile of activation of the slow accelerated oxidation stage is always increasing than the appearance of the activity level of the rapid oxidation stage. At this stage, the energetic functional groups in coal rarely react with oxygen molecules, and more energy is needed to accelerate the oxidation of coal. In the phase of fast oxidation, with the increase of temperature, some inactive functional groups are transformed into active states, resulting in massive heat released during the coal oxidation process, resulting in a decrease in the energy-dissipating pile of activation compared with the slowly accelerated oxidation periods, and the apparent energy-dissipating pile of activation of the coal oxygen reaction continues to decrease. The surface activation energy of mudstone samples is less than that of raw coal. The slow accelerated oxidation period is 2.97, 6.83, 6.38, 14.62 kJ/mol eliminated than that of raw coal, and the rapid oxidation period is 0.28–4.23 kJ/mol less than raw coal. It shows that each stage is more prone to oxidation after adding mudstone, which makes the self-ignition tendency of coal lower.

The mechanism of the effect of adding mudstone on the LTO stage of coal

To analyze the influence of mudstone on the LTO stage of coal spontaneous combustion, the pore structure characteristics of coal and mudstone, the physical and chemical parameters of the LTO experiment of coal-rock mixture with different mass ratios, and the changes of oxidation kinetic parameters were compared. Combined with the basic parameters of coal and mudstone, the mechanism of mudstone on the LTO of coal was determined, as shown in Fig. 15. There is an interaction between coal and mudstone, which is mainly based on mutual promotion. Adding mudstone accelerates its oxygen consumption, accelerates the heat release of the sample, reduces the energy required for its oxidation process, and achieves the effect of mutual promotion. In the first stage, the early stage of oxidation is dominated by water evaporation, because mudstone contains water-absorbing minerals, which accelerates the evaporation of water in coal, exposes active sites and pores and cracks of coal surface reacting with oxygen, and reaches the stage of accelerated and rapid oxidation (stages II and III). Mudstone has a larger specific surface area and pore volume than coal. The pore size distribution of mudstone is more uniform and the surface roughness is greater. These surface pores provide a good material channel for the transport of oxygen molecules, accelerate the oxidation of active sites, and increase the concentration of active centers. The increase of active center concentration and its continuous conversion with oxygen-containing functional groups leads to the accumulation of coal heat and the continuous increase of coal temperature. It promotes the exothermic chemical reaction and accelerates the oxidation reaction (The heat release intensity increases), accelerating the process of coal oxidation, thereby increasing the spontaneous combustion tendency of coal.

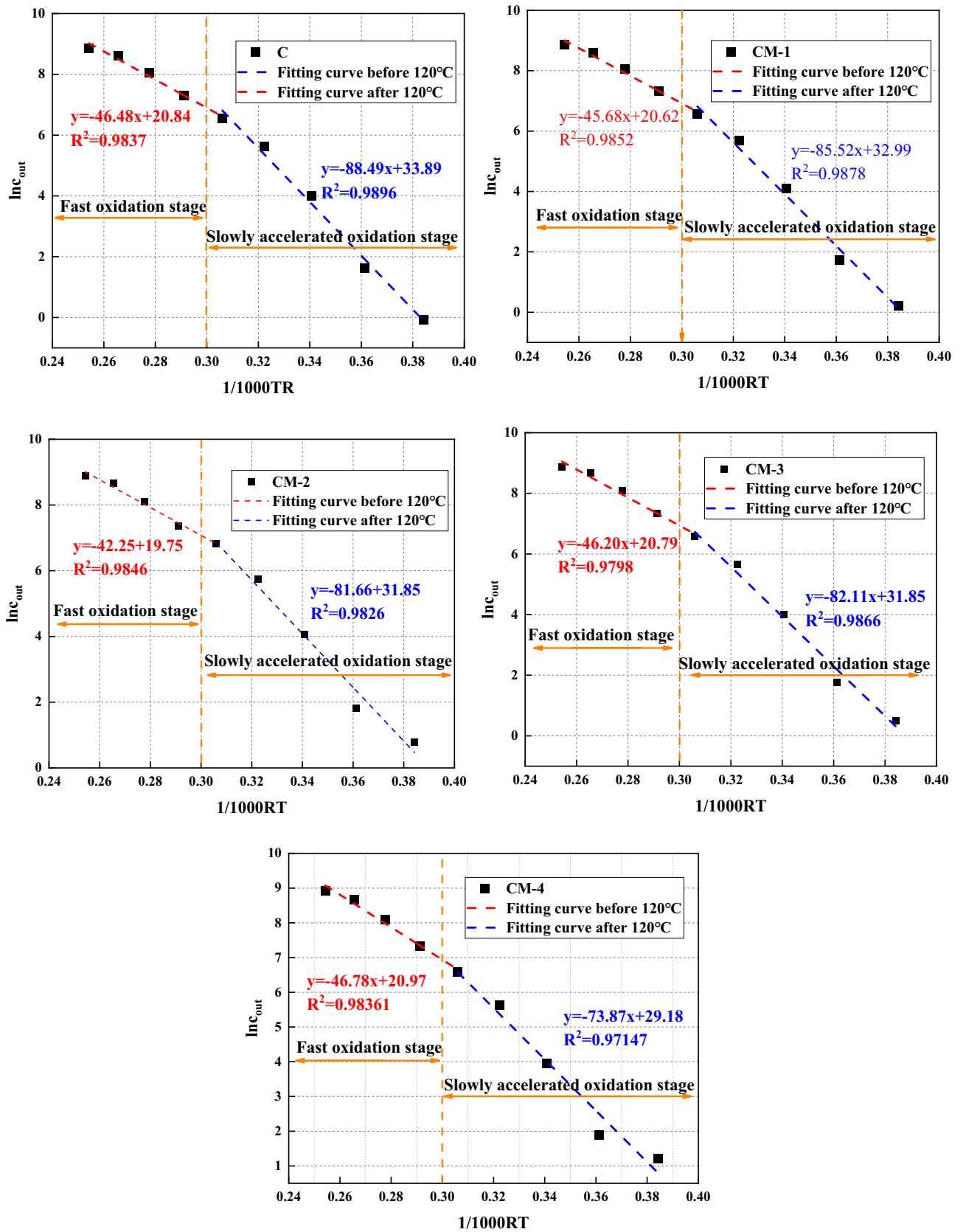


Figure 14. The results of apparent activation energy.

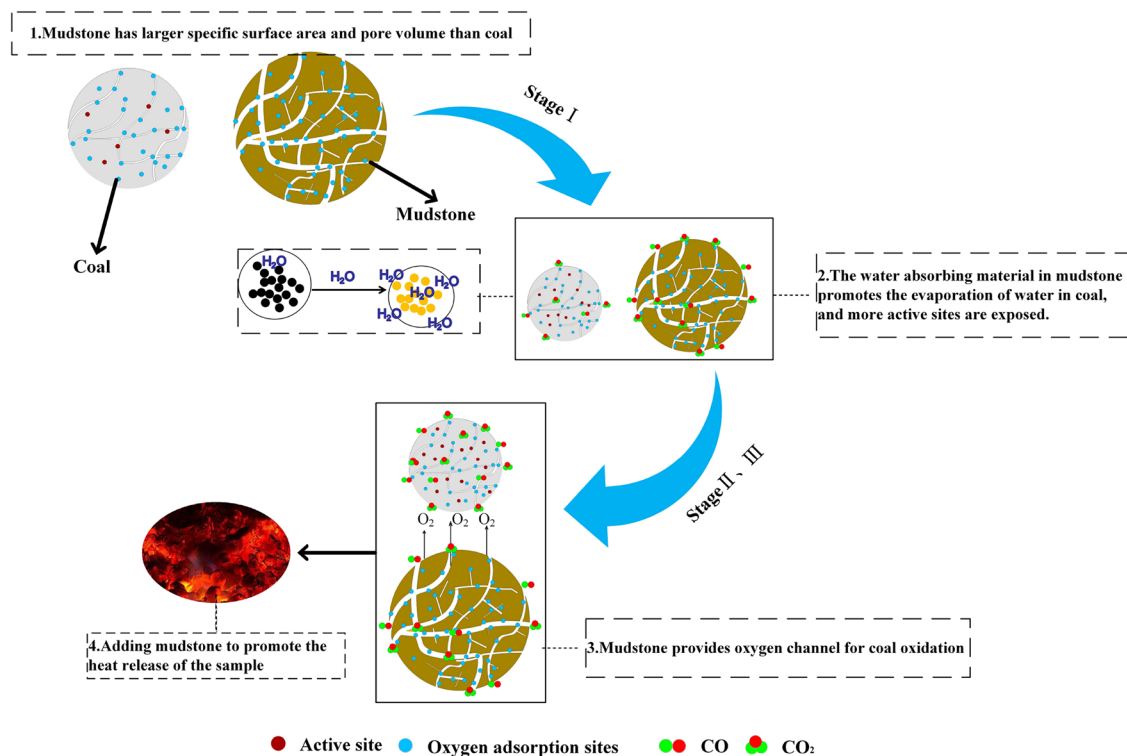


Figure 15. Mechanism of the effect of mudstone addition on the LTO process of coal.

Conclusion

Because of the effect of mudstone on the LTO process of coal, the physical parameters and oxidation kinetic parameters in the LTO process are analyzed by comparing the pore structure, specific surface area, and other related parameters of coal and mudstone. The main conclusions are as follows:

- (1) The specific surface area and pore volume of mudstone are 21.18 and 5.98 times that of coal, respectively. The pore size distribution of mudstone is more uniform. According to the fractal characteristics, the surface roughness of mudstone is larger and the pore structure is more complex, so mudstone can adsorb more gas.
- (2) With the increase of mudstone mass ratio, the amount of CO and CO₂ produced by the sample increases slightly, and the oxygen consumption rate increases. According to the comparison of theoretical and actual gas products and oxygen consumption rate, the difference is linearly related to the content of mudstone added. The results show that there is a mutual promotion effect between mudstone and coal in the LTO process, and the more mudstone content, the more obvious the promotion effect.
- (3) The exothermic intensity of coal-rock mixtures with different addition ratios was calculated. The highest exothermic intensity of CM-4 was $4533.9 \times 10^5 (\text{J cm}^{-3} \text{ s}^{-1})$, which was 1.33 times that of raw coal. The exothermic factor A and Greenham fire coefficient k increased with the increase of mudstone content, indicating that CM-4 had the most obvious effect on the exothermic promotion of the coal LTO process. The apparent activation energy of mudstone samples with different proportions is 2.97–14.62 kJ/mol lower than that of raw coal, indicating that the oxidation reaction is more likely to occur in each stage after adding mudstone, which makes the spontaneous combustion tendency of coal lower. In summary, the addition of mudstone increases the spontaneous combustion tendency of coal in the LTO stage.

Data availability

The datasets used and/or analysed during the current study available from the corresponding author on reasonable request.

Received: 31 January 2024; Accepted: 15 April 2024

Published online: 28 April 2024

References

1. Wang, D. M. *Mine fires* (China University of Mining and Technology Press, 2008).
2. Deng, J., Li, B., Wang, K. & Wang, C. P. Research status and outlook on prevention and control technology of coal fire disaster in China. *Coal Sci. Technol.* **44**(10), 1–7 (2016).

3. Wen, H. *et al.* Progress and trend evaluation study on coal mine thermodynamic disasters in China. *Saf. Coal Mines* **47**(3), 172–174 (2016).
4. Lan, H., Chen, D. K. & Mao, D. B. Current status of deep mining and disaster prevention in China. *Coal Sci. Technol.* **44**(01), 39–46 (2016).
5. Deng, J., Zhao, J. Y. & Zhang, Y. N. Study on determination of coal spontaneous combustion characteristic temperature based on analysis method of index gas growth-rate. *Coal Sci. Technol.* **42**(7), 49–52 (2014).
6. Deng, J. *et al.* Kinetic analysis of the low temperature spontaneous oxidation combustion of the coal seams due to the different metamorphism extents. *J. Saf. Environ.* **21**(01), 94–100 (2021).
7. Yan, G. F., Huang, X. L. & Yan, Z. G. Research on exothermic and kinetic characteristics of low-temperature oxidation of preoxidized coal. *J. Mine Autom.* **48**(07), 135–141 (2022).
8. Ren, L. F. *et al.* Low-temperature exothermic oxidation characteristics and spontaneous combustion risk of pulverised coal. *Fuel* **252**, 238–245 (2019).
9. Zhang, L. J. *et al.* Study on the change of organic sulfur forms in coal during low-temperature oxidation process. *Fuel* **222**, 350–361 (2018).
10. Zhao, W. B. *et al.* Laws of low temperature oxidation of water immersed and dehydrated coal samples in Goaf. *Saf. Coal Mines* **50**(01), 43–47 (2019).
11. Xiao, Y., Li, D. J., Lv, H. F., Yin, L. & Chen, L. G. Low-temperature oxidation characteristics of ionic liquid treated coal. *Coal Convers.* **41**(06), 15–21 (2018).
12. Dai, G. L. Experimental study on coal low-temperature oxidation and oxygen-adsorption. *J. Liaoning Tech. Univ. (Nat. Sci.)* **02**, 172–175 (2008).
13. Zhong, X. X., Kan, L., Xin, H. H., Qin, B. T. & Dou, G. L. Thermal effects and active group differentiation of low-rank coal during low-temperature oxidation under vacuum drying after water immersion. *Fuel* **236**, 1204–1212 (2019).
14. Zhang, X. *et al.* Stage changes in the oxidizing properties of long-term water-soaked coal and analysis of key reactive groups. *Fuel* **358**, 130186 (2024).
15. Zhang, X. *et al.* Experimental and simulation study on hydroxyl group promoting low-temperature oxidation of active groups in coal. *Fuel* **340**, 127501 (2023).
16. Yoshiie, R., Onda, M., Ueki, Y. & Naruse, I. Oxygen chemisorption and low-temperature oxidation behaviors of sub-bituminous coal [J]. *J. Thermal Sci. Technol.* **14**(1), 500 (2019).
17. Li, J. H., Lu, W., Li, J. L., Liang, Y. L. & Li, Z. H. Mutual conversion of active sites and oxygen-containing functional groups during low-temperature oxidation of coal. *Energy* **272**, 127151 (2023).
18. Zhang, Y. L. *et al.* Modes and kinetics of CO₂ and CO production from low-temperature oxidation of coal. *Int. J. Coal Geol.* **140**, 1–8 (2015).
19. Meng, X. L. *et al.* Effect of active functional groups in coal on the release behavior of small molecule gases during low-temperature oxidation. *Energy* **273**, 127290 (2023).
20. Zhang, Y. N. *et al.* Study on evolution characteristics of thermal contribution functional groups in low temperature oxidation process of bituminous coal. *Fuel* **341**, 127683 (2023).
21. Fan, L. *et al.* Pore Structure evolution and fractal analysis of Shenhua non-caking coal during low-temperature oxidation. *Energy Sour. Part A Recov. Util Environ. Eff* **44**(3), 6856–6867 (2022).
22. He, Y. J. *et al.* Experimental investigation of the macroscopic characteristic parameters and microstructure of water-soaked coal during low-temperature oxidation. *J. Therm. Anal. Calorim.* **147**(17), 9711–9723 (2022).
23. Bu, Y. C. *et al.* Study on pore structure change and lean oxygen re-ignition characteristics of high-temperature oxidized water-immersed coal. *Fuel* **323**, 124346 (2022).
24. Li, M. *et al.* Thermodynamic variation law and influence mechanism of low-temperature oxidation of lignite samples with different moisture contents. *Energy* **262**, 125605 (2023).
25. Cai, J. W., Yang, S. Q., Zheng, W. C., Song, W. X. & Gupta, R. Dissect the capacity of low-temperature oxidation of coal with different metamorphic degrees. *Fuel* **292**, 120256 (2021).
26. Qin, L. *et al.* Quantitative characterization of the pore volume fractal dimensions for three kinds of liquid nitrogen frozen coal and its enlightenment to coalbed methane exploitation. *Energy* **263**, 125741 (2023).
27. Mastalerz, M., Hampton, L., Drobniak, A. & Loope, H. Significance of analytical particle size in low-pressure N₂ and CO₂ adsorption of coal and shale. *Int. J. Coal Geol.* **178**, 122–131 (2017).
28. Sing, K. S. W. *et al.* Reporting physisorption data for gas/solid systems with special reference to the determination of surface area and porosity (Recommendations 1984). *Pure Appl. Chem.* **57**, 603–619 (1985).
29. Song, B. B. *et al.* Effect of water immersion on pore structure of bituminous coal with different metamorphic degrees. *Energy* **274**, 127449 (2023).
30. Wang, Z. Y. *et al.* Characteristics of microscopic pore structure and fractal dimension of bituminous coal by cyclic gas adsorption/desorption: An experimental study. *Fuel* **232**, 495–505 (2018).
31. Jablonska, B., Kityk, A. V., Busch, M. & Huber, P. The structural and surface properties of natural and modified coal gangue. *J. Environ. Manag.* **190**, 80–90 (2017).
32. Fu, H. J. *et al.* Characteristics of pore structure and fractal dimension of low-rank coal: A case study of Lower Jurassic Xishanyao coal in the southern Junggar Basin. *NW China. Fuel* **193**, 254–264 (2017).
33. Zhang, S. H. *et al.* Determining fractal dimensions of coal pores by FHH model: Problems and effects. *J. Nat. Gas Sci. Eng.* **21**, 929–939 (2014).
34. Li, Z. *et al.* Effect of ionic liquid treatment on pore structure and fractal characteristics of low rank coal. *Fuel* **262**, 116513 (2020).
35. Wang, Z. W., Lu, S. F., Wang, M. & Tian, S. S. Fractal characteristics of lacustrine shale and marine shale. *Lithologic Reserv.* **28**(01), 88–93 (2016).
36. Zhao, L. Y. *et al.* Pore characteristic and its influencing factors of Longtan shale in Dahebian syncline, Liupanshui coalfield, western Guizhou. *Nat. Gas Geosci.* **1**, 1–17 (2023).
37. Dai, J. W. *et al.* Limiting pathways and breakthrough pressure for CO₂ flow in mudstones. *J. Hydrol.* **625**, 129998 (2023).
38. Zhang, X. *et al.* Experimental study on effect of mudstone on spontaneous combustion of coal. *Energy* **285**, 128784 (2023).
39. Shi, Q. L., Jiang, W. J., Qin, B. T., Hao, M. Y. & He, Z. Y. Effects of oxidation temperature on microstructure and spontaneous combustion characteristics of coal: A case study of Shendong long-flame coal. *Energy* **284**, 128631 (2023).
40. He, M. C., Zhou, L., Li, J. D., Wang, C. G. & Nie, W. Experimental research on hydrophilic characteristics of mudstone in deep well. *Chin. J. Rock Mech. Eng.* **199**(06), 1113–1120 (2008).
41. Ren, S. J. *et al.* Thermal properties of coal during low temperature oxidation using a grey correlation method. *Fuel* **260**, 116287 (2020).
42. Li, Z. J. *Investigation on the mechanism of spontaneous combustion of sulphide ores and the key technologies for preventing fire* (Central South University, 2007).
43. Wang, C. P. *et al.* Synergistic acceleration effect of coal spontaneous combustion caused by moisture and associated pyrite. *Fuel* **304**, 121458 (2021).
44. Li, J. H. *et al.* Examination of CO, CO₂ and active sites formation during isothermal pyrolysis of coal at low temperatures. *Energy* **185**, 28–38 (2019).

45. Yan, H. W. *et al.* Experimental investigation and evaluation of influence of oxygen concentration on characteristic parameters of coal spontaneous combustion. *Thermochim. Acta* **717**, 179345 (2022).
46. Liang, Y. T., Zhang, J., Wang, L. C., Luo, H. Z. & Ren, T. Forecasting spontaneous combustion of coal in underground coal mines by index gases: A review. *J. Loss Prev. Process Ind.* **57**, 208–222 (2019).
47. Wang, C. P. *et al.* Comprehensive index evaluation of the spontaneous combustion capability of different ranks of coal. *Fuel* **191**, 120087 (2021).
48. Zhong, X. X., Wang, D. M. & Yin, X. D. Test method of critical temperature of coal spontaneous combustion based on the temperature. *J. China Coal Soc.* **35**(S1), 128–131 (2010).
49. Zhong, X. X., Wang, D. M. & Yin, X. D. Kinetic analysis of the low temperature spontaneous oxidation combustion of the coal seams due to the different metamorphism extents. *J. Saf. Environ.* **21**(01), 94–100 (2021).

Acknowledgements

This work was supported by the National Natural Science Foundation of China (52074147), Excellent Youth Fund Project of Liaoning Natural Science Foundation (2023JH3/10200011), Liaoning Revitalization Talents Program (XLYC2203118) and the National Natural Science Foundation of China (52274204).

Author contributions

Zhang X: writing—original draft, supervision, funding acquisition, project administration. Zou JH: conceptualization, methodology, writing—review and editing, writing—original draft. Lu B: data curation, formal analysis. Bai G: visualization, formal analysis. Qiao L: formal analysis, writing—review and editing.

Competing interests

The authors declare no competing interests.

Additional information

Correspondence and requests for materials should be addressed to J.Z.

Reprints and permissions information is available at www.nature.com/reprints.

Publisher's note Springer Nature remains neutral with regard to jurisdictional claims in published maps and institutional affiliations.



Open Access This article is licensed under a Creative Commons Attribution 4.0 International License, which permits use, sharing, adaptation, distribution and reproduction in any medium or format, as long as you give appropriate credit to the original author(s) and the source, provide a link to the Creative Commons licence, and indicate if changes were made. The images or other third party material in this article are included in the article's Creative Commons licence, unless indicated otherwise in a credit line to the material. If material is not included in the article's Creative Commons licence and your intended use is not permitted by statutory regulation or exceeds the permitted use, you will need to obtain permission directly from the copyright holder. To view a copy of this licence, visit <http://creativecommons.org/licenses/by/4.0/>.

© The Author(s) 2024